

RESEARCH ARTICLE

Synthesis and biological evaluation of biguanide and dihydrotriazine derivatives as potential inhibitors of dihydrofolate reductase of opportunistic microorganisms

Seema Bag¹, Nilesh R. Tawari¹, Sherry F. Queener², and Mariam S. Degani¹

¹Department of Pharmaceutical Sciences and Technology, Institute of Chemical Technology, Nathalal Parekh Marg, Matunga, Mumbai, India, and ²Department of Pharmacology and Toxicology, School of Medicine, Indiana University, Indianapolis, IN, USA

Abstract

Twenty-one biguanide and dihydrotriazine derivatives were synthesized and evaluated as inhibitors of dihydrofolate reductase (DHFR) from opportunistic microorganisms: *Pneumocystis carinii* (pc), *Toxoplasma gondii* (tg), *Mycobacterium avium* (ma), and rat liver (rl). The most potent compound in the series was **B2-07** with 12 nM activity against tgDHFR. The most striking observation was that **B2-07** showed similar potency to trimetrexate, ~233-fold improved potency over trimethoprim and ~7-fold increased selectivity as compared to trimetrexate against tgDHFR. Molecular docking studies in the developed homology model of tgDHFR rationalized the observed potency of **B2-07**. This molecule can act as a good lead for further design of molecules with better selectivity and improved potency.

Keywords: Biguanide; dihydrotriazine; dihydrofolate reductase

Introduction

The crucial reaction of conversion of folic acid to dihydro- and tetrahydro-folic acids (cofactor involved in one carbon donation in purine and pyrimidine *de novo* synthesis) is catalyzed by an NADPH (reduced nicotinamide adenine dinucleotide phosphate)-dependent enzyme dihydrofolate reductase (DHFR), which is found in both mammals and microorganisms. Inhibitors of DHFR interfere with the folate pathway that is crucial for cell growth and division, and have been in clinical use for over 50 years as anticancer, antibacterial, and antiprotozoal treatments. DHFR is present in both humans and microorganisms, and thus structural requirements for DHFR inhibition are of importance in designing potent analogs. The structural requirements for potential DHFR inhibitors are summarized in recent review articles^{1,2}.

Opportunistic organisms such as *Pneumocystis carinii* (pc), *Toxoplasma gondii* (tg), and *Mycobacterium avium* (ma) cause life-threatening infections in immunocompromised hosts³. DHFR inhibitors with high potency and selectivity are desired for the treatment of infections caused by

these pathogenic organisms. Several inhibitors with good potency are reported in the literature, but the optimum balance of potency and selectivity remains a major obstacle in this area due to the overall homology between mammalian and microbial DHFR. Several laboratories are continuing the search for agents that are potent and selective for microbial DHFR versus mammalian DHFR⁴⁻⁶. Very recently, Martucci *et al.* reported the identification of a non-active site inhibitor of *Cryptosporidium hominis* TS-DHFR by a virtual screen⁷.

Biguanide and dihydrotriazine derivatives have been successfully explored as DHFR inhibitors in the treatment of malaria, but there are very few reports on the usage of these molecules as pc-, tg-, and maDHFR inhibitors^{6,8}. Furthermore, most of the reported biguanides and dihydrotriazines in the literature are aromatic biguanide/dihydrotriazines with small substitutions on the aromatic ring. Kidwai *et al.*⁹ reported microwave assisted synthesis of 1-aryl-4,6-diamino-1,2-dihydrotriazines as antimalarial. Baker and Janson¹⁰ reported dihydrotriazine derivatives as inhibitors of mammalian DHFR. Lee and Chui¹¹ reported combinatorial synthesis and inhibitory activity of

Address for Correspondence: Professor Mariam Degani PhD, Department of Pharmaceutical Sciences and Technology, Institute of Chemical Technology, Nathalal Parekh Marg, Matunga, Mumbai, 400019 India. E-mail: msdegani@udct.org

(Received 12 March 2009; revised 15 May 2009; accepted 27 May 2009)

ISSN 1475-6366 print/ISSN 1475-6374 online © 2010 Informa UK Ltd
DOI: 10.3109/14756360903179443

<http://www.informahealthcare.com/enz>



dihydrophenyltriazine derivatives against rat liver DHFR. Mayer *et al.*¹² reported combinatorial library synthesis of biguanide derivatives as *Escherichia coli* DHFR inhibitors.

Only a few reports are available in the literature for derivatives with larger substituents at the aromatic biguanide/dihydrotriazine moiety. Jensen *et al.*¹³ reported the synthesis and antimalarial activity of phenoxypropoxybiguanides, and they also reported activity of PS-15 against ma- and pcDHFR. Queener *et al.*^{14,15} reported the screening of several compounds including some dihydrotriazines from the National Cancer Institute repository against tgDHFR and pcDHFR.

Derivatives possessing larger substituents (i.e. spacer sequences with polar end groups) are observed to reach additional binding sites of the DHFR. This was first shown by Kuyper *et al.*¹⁶ for 2,4-diamino-5-benzylpyrimidines bearing long-chain fatty acids, in which the carboxylate group could reach and interact with Arg57 of the active center of *E. coli* DHFR. This design concept was successfully utilized by Rosowsky *et al.*¹⁷ for 2,4-diaminopyrimidines and piritrexim analogs for the discovery of several selective molecules against pc-, tg-, and maDHFR. Based on a similar principle of design, Otzen *et al.*¹⁸ synthesized and evaluated several 2,4-diaminopyrimidine derivatives with the phthalimide moiety connected by a spacer to the ether oxygen in the 4-position of the benzyl ring of trimethoprim.

In the continued search for newer opportunistic DHFR inhibitors¹⁹ we herein report a series of molecules designed by joining the aromatic biguanide/dihydrotriazine moiety and phthalimide moiety (**A1** and **A2**) by the ether tether. Furthermore, various substitutions were made on the aromatic biguanide/dihydrotriazine moiety to probe the bulk and electronic tolerance of the binding pocket of the enzyme (**A2** and **B2**), as seen in the case of DHFR inhibitors such as **PS-15** and **WR-99210**¹³. The designed compounds were synthesized and evaluated as potential pc-, tg-, and maDHFR inhibitors.

Experimental

Materials and methods

General considerations

Melting points were recorded on a Campbell Electronics Thermomix apparatus, having an oil-heating system, and were uncorrected. The microwave reactions were carried out using a CEM Discover focused microwave system in monomode. Fourier transform infrared (FTIR) spectra were recorded on a Buck Scientific M500 IR spectrophotometer using KBr pellets. All nuclear magnetic resonance (NMR) spectra were recorded on a Jeol FT-NMR 60 MHz or Jeol AL 300 MHz spectrometer or Bruker DMX-500 spectrometer operating at 500 MHz, with dimethylsulfoxide (DMSO)-*d*₆ or CDCl₃ as solvent, using tetramethylsilane (TMS) as internal reference: s = singlet, d = doublet, t = triplet, q = quartet, m = multiplet, br = broad. Mass spectra (MS) were recorded on a Waters Q-ToF micromass spectrometer. All reagents and chemicals used were of "reagent grade."

Chemistry

General procedure for etherification reaction

To a refluxing mixture of 4-nitrophenol and base in an appropriate solvent was added freshly distilled alkyl/aryl halide. After refluxing the reaction mixture for 20–25 h the unreacted alkyl/aryl halide was isolated by distillation under reduced pressure. The resulting reaction mixture was dissolved in an organic solvent. The organic solvent was washed with 10% aqueous NaOH, to remove unreacted *p*-nitrophenol. The organic layer was washed with water till neutral to pH paper. The organic layer was then washed with brine and dried over anhydrous Na₂SO₄. Column purification yielded the desired product.

Representative example: synthesis of 1-(3-bromopropoxy)-4-nitrobenzene. To a refluxing solution of 4-nitrophenol (2 g, 0.014 mol) and K₂CO₃ (2.98 g, 0.021 mol) in acetonitrile (20 mL) was added freshly distilled 1,3-dibromopropane (4.35 g, 0.021 mol). The reaction mixture was refluxed for 20 h. On completion of reaction the unreacted 1,3-dibromopropane was isolated by distillation under reduced pressure. The resulting reaction mixture was dissolved in chloroform (10 mL) followed by washing with 20% NaOH. The organic layer was washed with water followed by brine and dried over anhydrous Na₂SO₄. Column purification (ethylacetate:*n*-hexane, 2:8) gave a white solid, 2.9 g (80% yield) of the desired product. IR (KBr) major bands at 3114, 2956, 1594, 1345, 1255, 1110, 1060, 920, 649 cm⁻¹; ¹H-NMR (60 MHz, CDCl₃) δ 8.29–8.14 (d, 2H, Ar-H, *J* = 9 MHz), 7.05–6.90 (d, 2H, Ar-H, *J* = 9 MHz), 4.32–4.13 (t, 2H, -CH), 3.72–3.51 (t, 2H, -CH), 2.56–2.17 (m, 2H, -CH).

General procedure for phthalimide condensation

The product obtained from the previous step and potassium phthalimide were dissolved in DMSO/dimethylformamide (DMF) and subjected to microwave irradiation under power 90 for 1 min with the target temperature set to 120°C. Cooling the resultant reaction mixture to room temperature followed by adding it to cold water with continuous stirring gave the desired product.

Representative example: 2-[3-(4-nitrophenoxy)propyl]-1H-isoindole-1,3(2H)-dione. The solution of 4-nitrophenoxypropyl bromide (1 g, 0.0038 mol) (isolated from step 1) and potassium phthalimide (0.70 g, 0.0038 mol) in DMSO (5 mL) was subjected to microwave irradiation under power 90 for 1 min with the target temperature set to 120°C. Addition of water to the reaction mixture followed by filtration and drying gave a pale white solid, 1.12 g (90% yield) of the desired product. mp 183–185°C; IR (KBr) major bands at 3455, 3113, 2937, 1768, 1707, 1593, 1504, 1335, 1262, 1109, 1060 cm⁻¹; ¹H-NMR (60 MHz, CDCl₃) δ 7.77–8.23 (m, 6H, Ar-H), 6.92–6.77 (d, 2H, Ar-H, *J* = 9 MHz), 4.23–3.82 (m, 4H, -CH), 2.43–2.03 (m, 2H, -CH).

General procedure for nitro reduction

The ethanolic solution of the product obtained from the previous step was refluxed with granulated tin in the

presence of concentrated HCl till completion of reaction. Then the reaction mixture was concentrated to half of its initial volume leading to precipitation of the desired product, which was collected by filtration and used for the next step.

Representative example: 2-[3-(4-aminophenoxy)propyl]-1*H*-isoindole-1,3(2*H*)-dione. To the ethanolic solution of 2-[3-(4-nitrophenoxy)propyl]-1*H*-isoindole-1,3(2*H*)-dione (1 g, 0.00306 mol) were added tin granules (0.54 g, 0.0046 mol). The reaction mixture was refluxed for 15 min followed by the addition of 1 mL concentrated HCl. The reaction mixture became clear after 3–4 h of reflux. After completion of reaction, the product was isolated as the hydrochloride salt. Drying gave a white solid, 0.92 g (90% yield) of the desired product. mp 238–239°C, IR (KBr) major bands at 3435, 2553, 1768, 1708, 1513, 1248, 1202, 1109, 1062 cm⁻¹; ¹H-NMR (60 MHz, CDCl₃) δ 7.89–7.85 (s, 4H, Ar-H), 6.72 (m, 4H, Ar-H), 4.10–3.88 (m, 4H, -CH), 2.92 (s, 2H, D₂O exchangeable -NH), 2.33–2.12 (m, 2H, -CH).

General procedure for biguanide and triazine derivative synthesis

The product obtained from the previous step was dissolved in ethanol and/or acetone. Dicyandiamide was added to it and the reaction mixture was refluxed for 18–20 h. The reaction mixture was adsorbed on silica gel and column purification led to the desired biguanide/triazine derivative.

Representative example: *N*-{4-[3-(1,3-dioxo-1,3-dihydro-2*H*-isoindol-2-yl)propoxy]phenyl}imidodicarbonimidic diamide hydrochloride (A1-02). The ethanolic solution of the hydrochloride salt of 2-[3-(4-aminophenoxy)propyl]-1*H*-isoindole-1,3(2*H*)-dione (0.2 g, 0.00060 mol) and dicyanamide (0.050 g, 0.00060 mol) was refluxed for 15–20 h. Concentration of the reaction mixture followed by column purification gave a yellow solid, 60 mg (25% yield) of the desired product.

Representative example: synthesis of 1-{4-[2-(1,3-dioxo-1,3-dihydro-2*H*-isoindol-2-yl)propoxy]phenyl}-6,6-dimethyl-1,6-dihydro-1,3,5-triazine-2,4-diamine hydrochloride (A2-02). The mixture of the hydrochloride salt of 2-[3-(4-aminophenoxy)propyl]-1*H*-isoindole-1,3(2*H*)-dione (0.2 g, 0.00060 mol) and dicyanamide (0.050 g, 0.00060 mol) in acetone was refluxed for 18–20 h. Filtration of the reaction mixture followed by washing with cold ethanol gave a white solid, 160 mg (59% yield) of the desired product.

All the designed biguanide and dihydrotriazine derivatives were synthesized using the general procedure as described above and were characterized spectroscopically.

N-{4-[2-(1,3-Dioxo-1,3-dihydro-2*H*-isoindol-2-yl)ethoxy]phenyl}imidodicarbonimidic diamide hydrochloride (A1-01). Light brown solid; mp 207°C; ¹H-NMR (DMSO, 500 MHz) δ: 9.31 (s, 1H, D₂O exchangeable -NH₃⁺), 7.87–7.83 (m, 4H, Ar-H), 7.17–7.16 (d, 2H, Ar-H, *J* = 9 MHz), 7.11 (s, 3H, D₂O exchangeable -NH₂), 6.94 (s, 2H, D₂O exchangeable -NH₂), 6.76–6.74 (d, 2H, Ar-H, *J* = 9 MHz), 3.98–3.96 (t, 2H, -CH), 3.77–3.74 (t, 2H, -CH); MS: 367.30 [M - Cl]⁺.

2-(2-(4-(4,6-Diamino-2,2-dimethyl-1,3,5-triazin-1(2*H*)-yl)phenoxy)ethyl)isoindoline-1,3-dione hydrochloride (A2-01). Light brown solid; mp 206°C. IR (KBr) major bands at 3405, 1773, 1701, 1631, 1228 cm⁻¹; ¹H-NMR (DMSO, 300 MHz) δ: 8.80 (s, 1H, D₂O exchangeable -NH₃⁺), 8.20 (s, br, 1H, D₂O exchangeable -NH₂), 7.81 (m, 4H, Ar-H), 7.60 (s, br, 1H, D₂O exchangeable -NH₂), 7.21 (d, 2H, Ar-H), 7.02 (d, 2H, Ar-H), 6.21 (s, br, 1H, D₂O exchangeable -NH₂), 4.22 (t, 2H, -CH), 4.02 (t, 2H, -CH), 1.21 (s, 6H, -CH₃); MS: 407.48 [M - Cl]⁺.

N-{4-[3-(1,3-Dioxo-1,3-dihydro-2*H*-isoindol-2-yl)propoxy]phenyl}imidodicarbonimidic diamide hydrochloride (A1-02). Yellow solid; mp 204–205°C; IR (KBr) major bands at 3310, 3196, 2916, 2875, 2584, 1764, 1701, 1654, 1618, 1584, 1542, 1508, 1253 cm⁻¹; ¹H-NMR (DMSO, 300 MHz) δ: 9.51 (s, br, 1H, D₂O exchangeable -NH₃⁺), 7.84 (s, 4H, Ar-H), 7.20–7.17 (m, 2H, Ar-H; 4H, D₂O exchangeable -NH₂), 6.75–6.72 (d, 2H, Ar-H, *J* = 8.7 MHz), 3.97 (t, 2H, -CH), 3.79–3.74 (t, 2H, -CH), 2.09–2.05 (m, 2H, -CH); MS: 381.40 [M - Cl]⁺.

2-(3-(4-(4,6-Diamino-2,2-dimethyl-1,3,5-triazin-1(2*H*)-yl)phenoxy)propyl)isoindoline-1,3-dione hydrochloride (A2-02). Light brown solid; mp 209°C; IR (KBr) major bands at 3467, 2366, 2335, 2195, 2159, 1773, 1716, 1627, 1560, 1249, 1161 cm⁻¹; ¹H-NMR (DMSO, 300 MHz) δ: 8.93 (s, 1H, D₂O exchangeable -NH₃⁺), 7.84 (s, 4H, Ar -H), 7.62 (s, br, 1H, D₂O exchangeable -NH₂), 7.24–7.21 (d, 2H, Ar-H, *J* = 8.4 MHz), 6.95–6.92 (d, 2H, Ar-H, *J* = 8.4 MHz), 6.26 (s, br, 1H, D₂O exchangeable -NH₂), 4.07–4.03 (t, 2H, -CH), 3.77–3.73 (t, 2H, -CH), 2.11–2.02 (t, 2H, -CH), 1.29 (s, 6H, -CH₃); ¹³C-NMR (DMSO, 300 MHz): 168.10, 159.03, 157.55, 134.46, 131.78, 131.16, 127.19, 123.07, 115.68, 69.68, 35.03, 27.66, 27.25; MS: 421.53 [M - Cl]⁺.

N-{4-[3-(1,3-Dioxo-1,3-dihydro-2*H*-isoindol-2-yl)butoxy]phenyl}imidodicarbonimidic diamide hydrochloride (A1-03). White solid; mp 200°C; IR (KBr) major bands at 3471, 3341, 3196, 1772, 1707, 1650, 1534, 1397, 1245, 1043 cm⁻¹; ¹H-NMR (DMSO, 500 MHz) δ: 9.32 (s, br, 1H, D₂O exchangeable -NH₃⁺), 7.88–7.83 (m, 4H, Ar-H), 7.20–7.19 (d, 2H, Ar-H, *J* = 8.5 MHz), 7.11 (s, 3H, D₂O exchangeable -NH₂), 6.95 (s, 2H, D₂O exchangeable -NH₂), 6.87–6.85 (d, 2H, Ar-H, *J* = 9 MHz), 3.95–3.93 (t, 2H, -CH), 3.64–3.62 (t, 2H, -CH), 1.73–1.72 (m, 4H, -CH); MS: 395.40 [M - Cl]⁺.

2-(4-(4-(4,6-Diamino-2,2-dimethyl-1,3,5-triazin-1(2*H*)-yl)phenoxy)butyl)isoindoline-1,3-dione (A2-03). White solid; mp 195°C; IR (KBr) major bands at 3421, 3348, 1768, 1715, 1639, 1563, 1521, 1390, 1249, 1170, 1028 cm⁻¹; ¹H-NMR (DMSO, 300 MHz) δ: 8.78 (s, 1H, D₂O exchangeable -NH₃⁺), 7.85 (m, 4H, Ar-H), 7.62 (s, br, 1H, D₂O exchangeable -NH₂), 7.25 (d, 2H, Ar-H, *J* = 8.4 MHz), 7.00 (d, 2H, Ar-H, *J* = 8.4 MHz), 6.26 (s, br, 1H, D₂O exchangeable -NH₂), 4.00 (t, 2H, -CH), 3.65 (t, 2H, -CH), 2.05 (m, 2H, -CH), 1.78 (m, 2H, -CH), 1.25 (s, 6H, -CH₃); MS: 435.51 [M - Cl]⁺.

2-(3-(4-(4,6-Diamino-2,2-dimethyl-1,3,5-triazin-1(2*H*)-yl)phenoxy)-2-hydroxypropyl)isoindoline-1,3-dione hydrochloride (A2-04). Brown colored solid; mp 223°C; ¹H-NMR (DMSO, 500 MHz) δ: 8.78 (s, 1H, D₂O exchangeable -NH₃⁺),

7.89–7.84 (m, 4H, Ar-H), 7.62 (s, br, 1H, D₂O exchangeable -NH₂), 7.28–7.26 (d, 2H, Ar-H, *J* = 8 MHz), 7.04–7.02 (d, 2H, Ar-H, *J* = 8 MHz), 6.29 (s, br, 1H, D₂O exchangeable -NH₂), 4.23–4.16 (m, 1H, -CH), 4.03–4.01 (m, 2H, -CH), 3.76–3.71 (m, 2H, -CH), 3.08 (s, br, 1H, D₂O exchangeable -OH), 1.32 (s, 6H, -CH₃); MS: 437.40 [M - Cl]⁺.

N-[4-(Benzyloxy)phenyl]imidodicarbonimidic diamide hydrochloride (B1-01). White solid; mp 242 °C; ¹H-NMR (DMSO, 500 MHz) δ: 9.42 (s, 1H, D₂O exchangeable -NH₃⁺), 8.11 (s, br, 1H, D₂O exchangeable -NH₂), 7.73 (s, br, 3H, D₂O exchangeable -NH₂), 7.44–7.32 (m, 5H, Ar-H), 7.23–7.22 (d, 2H, Ar-H, *J* = 8 MHz), 6.97–6.95 (m, 2H, Ar-H), 5.07 (s, 2H, -CH); MS: 284.32 [M - Cl]⁺.

1-(4-(Benzyloxy)phenyl)-6,6-dimethyl-1,6-dihydro-1,3,5-triazine-2,4-diamine hydrochloride (B2-01). White solid; mp 215 °C; IR (KBr) 3425, 3342, 1641, 1555, 1488, 1250, 1171 cm⁻¹; ¹H-NMR (DMSO, 300 MHz) δ: 8.82 (s, 1H, D₂O exchangeable -NH₃⁺), 7.62 (s, br, 1H, D₂O exchangeable -NH₂), 7.50–7.30 (m, 5H, Ar-H), 7.30 (d, 2H, Ar-H, *J* = 9 MHz), 7.15 (d, 2H, Ar-H, *J* = 9 MHz), 6.30 (s, br, 1H, D₂O exchangeable -NH₂), 5.10 (s, 2H, -CH), 1.30 (s, 6H, -CH₃); MS: 324.45 [M - Cl]⁺.

N-{4-[(3-Chlorobenzyl)oxy]phenyl}imidodicarbonimidic diamide hydrochloride (B1-02). Light brown solid; mp 208–209 °C; IR (KBr) major bands at 3466, 3366, 3186, 1649, 1541, 1509, 1420, 1228, 829, 782 cm⁻¹; ¹H-NMR (DMSO, 500 MHz) δ: 9.62 (s, br, 1H, D₂O exchangeable -NH₃⁺), 7.79 (s, br, 1H, D₂O exchangeable -NH₂), 7.50 (s, 1H, D₂O exchangeable -NH₂), 7.44–7.38 (m, 2H, Ar-H), 7.25–7.21 (m, 4H, Ar-H; 1H, D₂O exchangeable -NH₂), 7.03 (s, 2H, D₂O exchangeable -NH₂), 6.97–6.95 (m, 2H, Ar-H), 5.09 (s, 2H, -CH); MS: 318.27 [M - Cl]⁺.

1-(4-(3-Chlorobenzyl)oxy)phenyl)-6,6-dimethyl-1,6-dihydro-1,3,5-triazine-2,4-diamine hydrochloride (B2-02). White solid; mp 207 °C; IR (KBr) major bands at 3440, 3347, 1641, 1555, 1519, 1483, 1249, 834 cm⁻¹; ¹H-NMR (DMSO, 300 MHz) δ: 8.80 (s, 1H, D₂O exchangeable -NH₃⁺), 7.60 (s, br, 1H, D₂O exchangeable -NH₂), 7.40–7.50 (m, 4H, Ar-H), 7.30 (d, 2H, Ar-H, *J* = 9 MHz), 7.15 (d, 2H, Ar-H, *J* = 8.9 MHz), 6.30 (s, br, 1H, D₂O exchangeable -NH₂), 5.10 (s, 2H, -CH), 1.30 (s, 6H, -CH₃); MS: 358.34 [M - Cl]⁺.

N-{4-[(2-Chlorobenzyl)oxy]phenyl}imidodicarbonimidic diamide hydrochloride (B1-03). Brown solid; mp 190 °C; ¹H-NMR (DMSO, 500 MHz) δ: 9.42 (s, br, 1H, D₂O exchangeable -NH₃⁺), 8.15 (s, br, 1H, D₂O exchangeable -NH₂), 7.74 (s, br, 1H, D₂O exchangeable -NH₂), 7.59–7.58 (m, 1H, Ar-H), 7.52–7.50 (m, 1H, Ar-H), 7.41–7.38 (m, 2H, Ar-H), 7.26–7.24 (d, 2H, Ar-H, *J* = 9 MHz), 7.16 (s, 2H, Ar-H; 2H, D₂O exchangeable -NH₂), 5.12 (s, 2H, -CH); MS: 318.27 [M - Cl]⁺.

1-(4-(2-Chlorobenzyl)oxy)phenyl)-6,6-dimethyl-1,6-dihydro-1,3,5-triazine-2,4-diamine hydrochloride (B2-03). Buff solid; mp 196 °C; ¹H-NMR (DMSO, 300 MHz) δ: 9.30 (s, 1H, D₂O exchangeable -NH₃⁺), 7.60 (m, 1H, Ar-H), 7.50 (m, 1H, Ar-H), 7.40 (m, 2H, Ar-H; 2H, D₂O exchangeable -NH), 7.30 (d, 2H, Ar-H, *J* = 8.9 MHz), 7.15 (d, 2H, Ar-H, *J* = 8.9 MHz), 6.30 (s, br, 1H, D₂O exchangeable -NH₂), 5.20 (s, 2H, -CH), 1.30 (s, 6H, -CH₃); MS: 358.34 [M - Cl]⁺.

N-{4-[(2,4-Dichlorobenzyl)oxy]phenyl}imidodicarbonimidic diamide hydrochloride (B1-04). White solid; mp 204 °C; ¹H-NMR (DMSO, 500 MHz) δ: 9.35 (s, br, 1H, D₂O exchangeable -NH₃⁺), 7.70–7.69 (d, 2H, Ar-H), 7.61–7.60 (d, 1H, Ar-H, *J* = 8 MHz), 7.49–7.47 (m, 1H, Ar-H), 7.25–7.24 (d, 2H, Ar-H, *J* = 9.5 MHz), 7.13 (s, br, 3H, D₂O exchangeable -NH₂), 7.00–6.96 (m, 1H, Ar-H; 2H, D₂O exchangeable -NH₂), 5.11 (s, 2H, -CH); MS: 352.29 [M - Cl]⁺.

1-(4-(2,4-Dichlorobenzyl)oxy)phenyl)-6,6-dimethyl-1,6-dihydro-1,3,5-triazine-2,4-diamine hydrochloride (B2-04). White solid; mp 209 °C; ¹H-NMR (DMSO, 300 MHz) δ: 8.95 (s, 1H, D₂O exchangeable -NH₃⁺), 7.70 (s, 1H, Ar-H; 1H, D₂O exchangeable -NH), 7.60 (m, 1H, Ar-H), 7.50 (m, 1H, Ar-H), 7.30 (d, 2H, Ar-H, *J* = 9 MHz), 7.15 (d, 2H, Ar-H, *J* = 9 MHz), 6.30 (s, br, 1H, D₂O exchangeable -NH₂), 5.20 (s, 2H, -CH), 1.30 (s, 6H, -CH₃); MS: 392.36 [M - Cl]⁺.

N-{4-[(4-Bromobenzyl)oxy]phenyl}imidodicarbonimidic diamide hydrochloride (B1-05). Brown solid; mp 144 °C; ¹H-NMR (DMSO, 500 MHz) δ: 9.43 (s, br, 1H, D₂O exchangeable -NH₃⁺), 7.60–7.57 (m, 2H, Ar-H), 7.41–7.39 (m, 2H, Ar-H), 7.24–7.22 (m, 2H, Ar-H), 7.15 (s, br, 3H, D₂O exchangeable -NH₂), 6.98 (s, br, 2H, D₂O exchangeable -NH₂), 6.96–6.94 (m, 2H, Ar-H), 5.05 (s, 2H, -CH); MS: 362.25 [M - Cl]⁺, 364.26, 365.33.

1-(4-(4-Bromobenzyl)oxy)phenyl)-6,6-dimethyl-1,6-dihydro-1,3,5-triazine-2,4-diamine hydrochloride (B2-05). White solid; mp 217 °C; ¹H-NMR (DMSO, 500 MHz) δ: 8.73 (s, 1H, D₂O exchangeable -NH₃⁺), 7.63–7.60 (m, 2H, Ar-H; 2H, D₂O exchangeable), 7.44–7.43 (d, 2H, Ar-H, *J* = 8 MHz), 7.31–7.28 (m, 2H, Ar-H), 7.15–7.12 (m, 2H, Ar-H; 1H D₂O exchangeable), 6.30 (s, br, 1H, D₂O exchangeable -NH), 5.12 (s, 2H, -CH), 1.32 (s, 6H, -CH₃); MS: 402.31 [M - Cl]⁺, 404.33 [M - Cl + 2]⁺.

N-{4-[(3-Methoxybenzyl)oxy]phenyl}imidodicarbonimidic diamide hydrochloride (B1-06). Light brown solid; mp 208 °C; IR (KBr) major bands at 3471, 3352, 3310, 3186, 1654, 1612, 1584, 1536, 1507, 1420, 1265, 1240, 1156 cm⁻¹; ¹H-NMR (DMSO, 300 MHz) δ: 9.80 (s, br, 1H, D₂O exchangeable -NH₃⁺), 7.20–7.25 (m, 3H, Ar-H; 3H, D₂O exchangeable -NH₂), 7.02 (s, br, 2H, D₂O exchangeable -NH₂), 6.81–7.00 (m, 5H, Ar-H), 5.02 (s, 2H, -CH), 3.78 (s, 3H, -OCH₃); MS: 314.37 [M - Cl]⁺.

1-(4-(4-Methoxybenzyl)oxy)phenyl)-6,6-dimethyl-1,6-dihydro-1,3,5-triazine-2,4-diamine hydrochloride (B2-06). Off-white solid; mp 204–205 °C; IR (KBr) major bands at 3414, 3342, 1636, 1558, 1522, 1245, 1164 cm⁻¹; ¹H-NMR (DMSO, 500 MHz) δ: 8.66 (s, 1H, D₂O exchangeable -NH₃⁺), 7.62 (s, br, 1H, D₂O exchangeable -NH), 7.40–7.39 (d, 2H, Ar-H, *J* = 8.5 MHz), 7.29–7.27 (d, 2H, Ar-H, *J* = 9 MHz), 7.13–7.11 (d, 2H, Ar-H, *J* = 9 MHz), 6.97–6.96 (d, 2H, Ar-H, *J* = 8.5 MHz), 6.15 (s, br, 1H, D₂O exchangeable -NH), 5.04 (s, 2H, -CH), 3.77–3.76 (s, 3H, -OCH₃), 1.32 (s, 6H, -CH₃); MS: 354.37 [M - Cl]⁺.

N-[4-(Biphenyl-4-ylmethoxy)phenyl]imidodicarbonimidic diamide hydrochloride (B1-07). White solid; mp 233 °C; ¹H-NMR (DMSO, 500 MHz) δ: 9.27 (s, br, 1H, D₂O exchangeable -NH₃⁺), 7.69–7.66 (m, 3H, Ar-H), 7.53–7.52 (d, 2H, Ar-H, *J* = 8 MHz), 7.48–7.45 (m, 2H, Ar-H), 7.39–7.36 (t, 1H, Ar-H),

7.37 (m, 2H, Ar-H), 7.11 (s, br, 3H, D₂O exchangeable -NH₂), 7.00–6.98 (m, 2H, Ar-H), 6.94 (s, br, 2H, D₂O exchangeable -NH₂), 5.13 (s, 2H, -CH); MS: 360.42 [M - Cl]⁺.

1-(4-(Biphenyl-4-ylmethoxy)phenyl)-6,6-dimethyl-1,6-dihydro-1,3,5-triazine-2,4-diamine hydrochloride (B2-07). White solid; mp 229°C; ¹H-NMR (DMSO, 300 MHz) δ: 8.79 (s, 1H, D₂O exchangeable -NH₃⁺), 7.72–7.67 (m, 4H, Ar-H), 7.64 (br, s, 1H, D₂O exchangeable -NH), 7.57–7.56 (m, 2H, Ar-H *J* = 7.5 MHz), 7.49–7.46 (m, 2H, Ar-H), 7.39–7.36 (m, 1H, Ar-H; 2H, D₂O exchangeable -NH), 7.32–7.30 (d, 2H, Ar-H, *J* = 8.5 MHz), 7.18–7.16 (d, 2H, Ar-H, *J* = 9 MHz), 6.25 (s, br, 1H, D₂O exchangeable -NH), 5.19 (s, 2H, -CH), 1.33 (s, 6H, -CH₃); MS: 400.49 [M - Cl]⁺.

Biological assay

The synthesized compounds were evaluated for their ability to inhibit DHFR from pc, tg, ma, and rl using a continuous spectrophotometric assay measuring oxidation at 340 nM of NADPH at 37°C under conditions of saturating substrate and cofactor as previously described^{14,15}.

Results and discussion

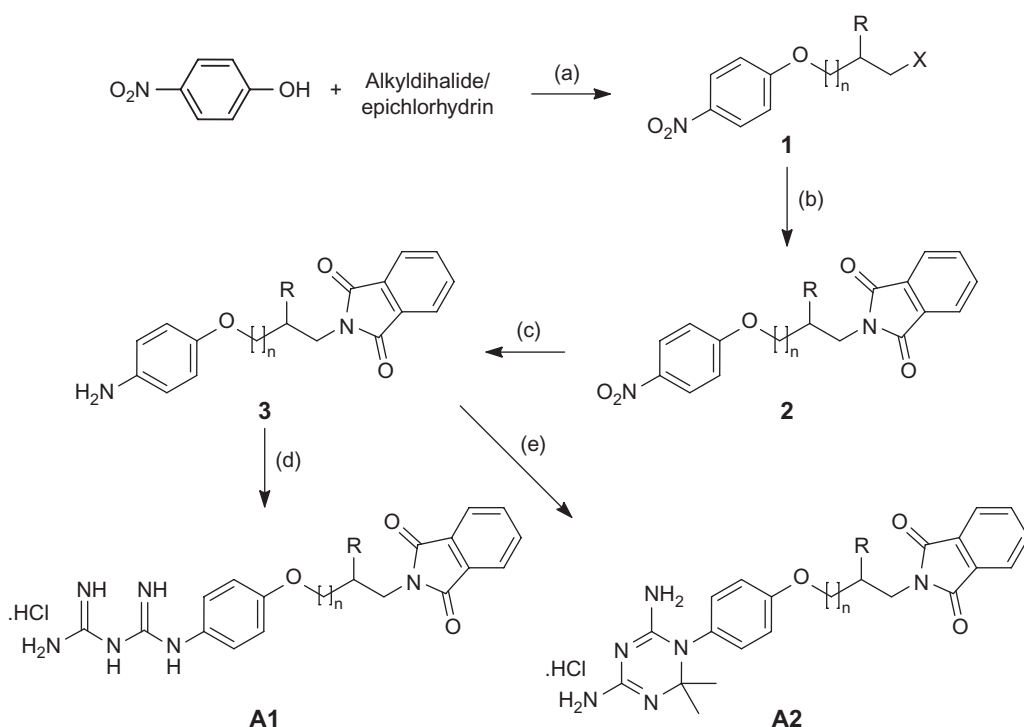
Chemistry

The target compounds were synthesized utilizing the reaction sequence as shown in Schemes 1 and 2. Etherification of *p*-nitrophenol was carried out with alkyl and benzyl halides to obtain **1** or **4**, respectively²⁰. Different alkyl and benzyl halides were used to create diversity in the series. The product **1** (from alkyldihalides or epichlorohydrin) was

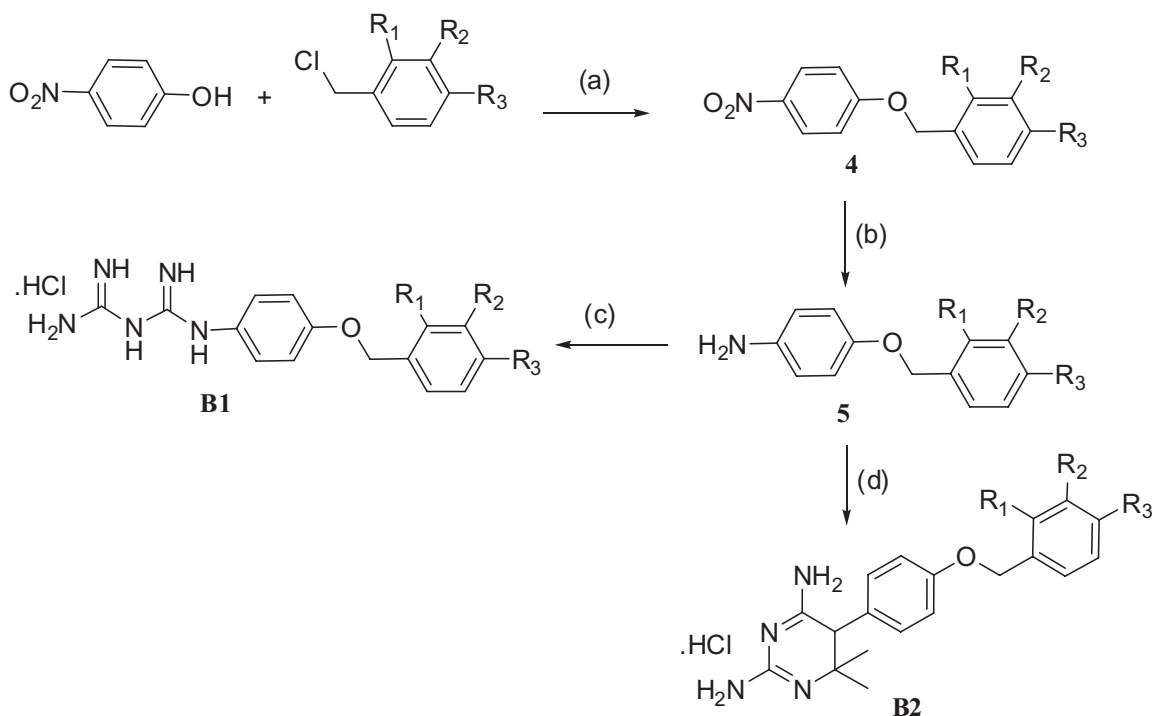
reacted with the potassium salt of phthalimide under microwave irradiation using DMSO as solvent (Scheme 1). The microwave (MW) assisted synthesis was advantageous over conventional reaction of 12 h reported in the literature²¹ with respect to time, yield, and workup procedures. The product **2** or **4** was reduced using Sn/HCl to obtain **3** or **5**, respectively. This step was followed by reaction with dicyandiamide to obtain biguanide derivatives **A1 (01-03)** or **B1 (01-07)**²². When **3** or **5** was treated with acetone and dicyandiamide it cyclized to give the corresponding dihydrotriazine derivative **A2 (01-04)** or **B2 (01-07)**^{22,23}. The course of the reaction was monitored by thin layer chromatography (TLC) and the structures were confirmed by spectral data. IR spectra showed the presence of a characteristic quaternary amine band at 3000–3550 cm⁻¹; characteristic carbonyl bands corresponding to two C=O groups were observed at ~1700 and 1775 cm⁻¹, in the case of compounds **A1 (01-03)** or **B1 (01-07)**. A sharp band corresponding to C=N stretching was observed at ~1384–1390 cm⁻¹ in all molecules synthesized. In most of the synthesized biguanide and dihydrotriazine derivatives ¹H-NMR spectra showed the proton of the quaternary amine at δ 9–9.5. MS of all the compounds exhibited the [M - Cl]⁺ peak. All other spectral data were found to be satisfactory in confirming their structures.

Structure activity relationship

The synthesized compounds were evaluated for their ability to inhibit DHFR from pc, tg, ma, and rl^{14,15}. Rat liver DHFR was used as the mammalian standard. The data for the reference compounds (trimethoprim, piritrexim, and trimetrexate) were taken from the study of Gangjee *et al.*³



Scheme 1. Scheme for the synthesis of **A1 (01-03)** and **A2 (01-04)**. (a) K₂CO₃, CH₃CN, reflux; (b) potassium salt of phthalimide, DMSO, MW, 70W, 120°C; (c) Sn/HCl, ethanol; (d) dicyandiamide, ethanol, reflux; (e) dicyandiamide, acetone, reflux.



Scheme 2. Scheme for the synthesis of **B1** (**01-07**) and **B2** (**01-07**). (a) K_2CO_3 , CH_3CN , reflux; (b) Sn/HCl , ethanol; (c) dicyandiamide, ethanol, reflux; (d) dicyandiamide, acetone, reflux.

for comparative purpose. IC_{50} values for all analogs are given in Table 1.

The dihydrotriazine derivatives were found to be more active than their corresponding biguanide derivatives. It was also observed that in the dihydrotriazine analogs, as the carbon chain length between rings B and C increased from 2 to 4 carbons, potency toward DHFR increased in all species, but selectivity declined. The introduction of hydrophilic groups such as hydroxyl in the carbon chain caused an approximately four- to six-fold decrease of biological activity compared to the corresponding unsubstituted analog as seen in compound **A2-02** vs. **A2-04**. Substitution of bulky groups and halogens at the meta and/or para position of C ring systems caused an increase in activity as compared to an unsubstituted phenyl ring in the C ring system, as seen in compounds **B2** (**01-07**) in pc- and maDHFR.

In the case of pcDHFR **B2-07**, the biphenyl derivative of dihydrotriazine was the most potent, having a 14-fold increase in activity as compared to the unsubstituted phenyl analog **B2-01**, and was more active than compounds with smaller substituents. However, one drawback was that none of the synthesized compounds were selective against pcDHFR.

The compounds showed high potency toward tgDHFR compared to pcDHFR. Particularly, of the 21 molecules synthesized, seven molecules **B2** (**01-07**) showed high potency with activity <50 nM toward tgDHFR. The most potent compound was again the biphenyl analog **B2-07**, which had an IC_{50} value of 12 nM. Some selectivity was observed toward tg- vs. rIDHFR for molecules **B2-01**, **A2-04**, **B1-05**, **A2-02**, **A2-01**, **B2-06**, **B2-07**, and **B1-03**. Molecule **B2-01** showed 32 nM activity against tgDHFR with a selectivity index of ~ 4 .

In the case of maDHFR, the most potent analog was **B2-06** with an IC_{50} of 3.383 μM . Bulky substitutions such as biphenyl were detrimental to activity against maDHFR, as seen from **B2-07** with an IC_{50} of 10.208 μM . There was no selectivity for maDHFR for this series of analogs.

Both biguanide and dihydrotriazine derivatives showed significant inhibition of rIDHFR. Compounds **A2-03** and **B2** (**02-07**) were potent nanomolar inhibitors of mammalian DHFR.

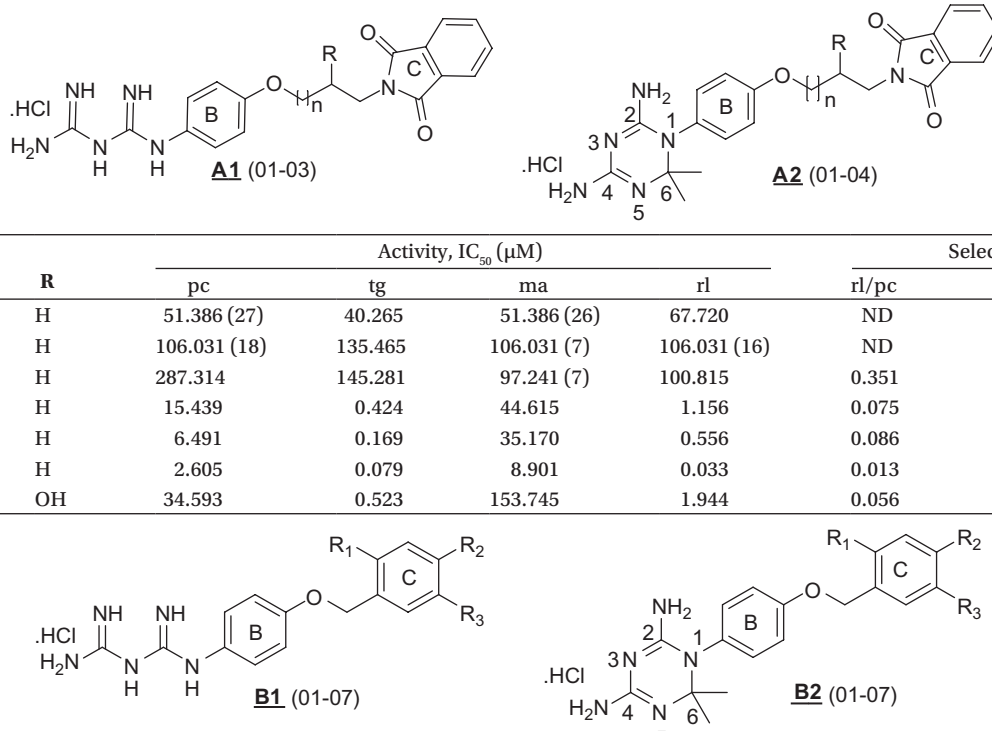
The comparison of biological activities of synthesized molecules with clinically used antifolates revealed that four of the 21 synthesized molecules (**B2-02**, **B2-04**, **B2-05**, and **B2-07**) showed >10 -fold potency compared with trimethoprim against pcDHFR. Similarly, three of the 21 synthesized molecules (**B2-02**, **B2-06**, and **B2-07**) showed >100 -fold potency compared with trimethoprim against tgDHFR. However, the improved potency was at the cost of decreased selectivity.

The most striking observation was that **B2-07** showed similar potency and ~ 7 -fold increased selectivity as compared to trimetrexate against tgDHFR. In order to understand the observed potency and to predict the binding mode of **B2-07**, molecular modeling studies were undertaken.

Molecular modeling

Molecular docking studies were carried out using the standard Glide molecular docking protocol implemented within the Maestro molecular modeling suite by Schrödinger, LLC, New York, NY, 2008 installed on an AMD Athlon workstation²⁴.

To understand the forms of interaction with the enzyme and to identify the binding mode of **B2-07**, molecular docking was carried out in the active site of the developed

Table 1. Inhibitory concentration (IC_{50} , μM) against rDHFR, pcDHFR, tgDHFR, and maDHFR and selectivity ratios versus rDHFR by target compounds.


Mol ID	<i>n</i>	R	Activity, IC_{50} (μM)				Selectivity index		
			pc	tg	ma	rl	rl/pc	rl/tg	rl/ma
A1-01	0	H	51.386 (27)	40.265	51.386 (26)	67.720	ND	1.682	ND
A1-02	1	H	106.031 (18)	135.465	106.031 (7)	106.031 (16)	ND	ND	ND
A1-03	2	H	287.314	145.281	97.241 (7)	100.815	0.351	0.694	ND
A2-01	0	H	15.439	0.424	44.615	1.156	0.075	2.724	0.0259
A2-02	1	H	6.491	0.169	35.170	0.556	0.086	3.287	0.0158
A2-03	2	H	2.605	0.079	8.901	0.033	0.013	0.422	0.0037
A2-04	1	OH	34.593	0.523	153.745	1.944	0.056	3.717	0.0126

Mol ID	R ₁	R ₂	R ₃	Activity, IC_{50} (μM)				Selectivity index		
				pc	tg	ma	rl	rl/pc	rl/tg	rl/ma
B1-01	H	H	H	131.649 (10)	131.649 (25)	131.649 (3)	131.649 (22)	ND	ND	ND
B1-02	H	H	Cl	103.914	58.464	63.771	68.740	0.662	1.176	1.078
B1-03	Cl	H	H	293.027	9.948	152.442 (30)	20.834	0.071	2.094	ND
B1-04	Cl	Cl	H	123.006	111.146 (19)	111.146 (16)	27.941	0.227	ND	ND
B1-05	H	Br	H	163.839	21.430	127.419 (36)	74.946	0.457	3.497	ND
B1-06	H	H	OCH ₃	15.522 (5)	8.404	15.522 (2)	14.716	ND	1.751	ND
B1-07	H	Ph	H	103.565 (24)	111.371	103.565 (3)	66.964	ND	0.601	ND
B2-01	H	H	H	5.399	0.032	14.411	0.120	0.022	3.801	0.0083
B2-02	H	H	Cl	1.109	0.020	4.081	0.034	0.031	1.738	0.0084
B2-03	Cl	H	H	2.531	0.040	10.348	0.073	0.029	1.841	0.0071
B2-04	Cl	Cl	H	1.076	0.029	11.240	0.018	0.017	0.627	0.0016
B2-05	H	Br	H	0.829	0.033	7.321	0.033	0.040	1.017	0.0045
B2-06	H	H	OCH ₃	1.689	0.019	3.383	0.048	0.029	2.551	0.0143
B2-07	H	Ph	H	0.403	0.012	10.208	0.026	0.064	2.151	0.0025
Trimethoprim ^a	—	—	—	12	2.80	0.30	180	14	65	600
Piritrexim ^a	—	—	—	0.013	0.0043	0.00061	0.0033	0.26	0.76	5.3
Trimetrexate ^a	—	—	—	0.042	0.01	0.0015	0.003	0.07	0.3	2.0

Note. Triplicate assays were performed as previously described^{14,15}. Number in parentheses indicates percent inhibition obtained at that concentration. Selectivity index: rl/pc, IC_{50} rDHFR/ IC_{50} pcDHFR; rl/tg, IC_{50} rDHFR/ IC_{50} tgDHFR; rl/ma, IC_{50} rDHFR/ IC_{50} maDHFR.

^aData taken from reference 3.

homology model of tgDHFR ("Homology modeling of tgDHFR," unpublished results). The bond orders and charges of cofactor NADPH and methotrexate were assigned in the protein preparation step using the protein preparation "wizard" in Maestro, and a grid representation of the shape and properties of the receptor using several different sets of fields was generated.

The ligand structure was constructed using the build option within Maestro employing standard geometries and

bond lengths. In the case of dihydrotriazine analogs the nitrogen N5 was protonated and given a positive charge, and the protonated structures were used for the docking study (Table 1). With the help of the LigPrep facility, appropriate hydrogens were added and a single, low-energy, 3D conformation was generated for the ligand by energy minimization using a Merck molecular force field (MMFF) with a dielectric constant of 1.0²⁵. The docking study was carried out using the extra precision (XP) mode with "must match" of at least one

hydrogen bond criterion: with Ile5, Val123, and Asp27, as these are the conserved residues in most of the DHFRs and H-bonding with these residues is one of the essential criteria for antifolate activity.

Figure 1 shows the predicted binding mode of **B2-01** in the active site of tgDHFR. It was noticeable that the dihydrotriazine ring system of **B2-01** positions itself at the bottom of the active site as seen in the case of the 2,4-diaminopteridine ring system for methotrexate. The diamino groups and protonated N5 of the dihydrotriazine ring system forms a hydrogen bond with Asp31, Val9, and Val151, while ring B is involved in the π - π stacking interaction with the nicotinamide ring of NADPH (centroid-centroid distance 4.163 Å). Methyl groups at the C6 position form van der Waals interactions with Leu23, Asp31, and Phe32. Ring C binds in the pocket formed by Phe32, Ser86, and Met87. The most noticeable observation was that the distal ring of the biphenyl part of the molecule is involved in the π - π stacking interaction with Phe91 (centroid-centroid distance 4.189 Å), thus making this molecule the most potent in the series.

For the comparison of docking scores with binding energies, the experimental IC_{50} values were converted to a free-energy scale via $\Delta G_{\text{expt}} = RT \ln IC_{50}$. Comparison of the docking scores and experimental free energies revealed that the scoring function is able to reproduce the experimental binding energy with ± 3 kcal/mol variation for 21 out of 24 compounds including trimethoprim, piritrexim, and trimetrexate. This is particularly significant considering the fact that docking studies were performed in the homology model (Table 2). Interestingly, the experimental binding energy value (-11.23 kcal/mol) of the most active compound was well predicted (-11.99 kcal/mol) by the Glide score, and it was correctly ranked as the most potent compound among the synthesized molecules. Thus, this validates both the homology model and the predicted binding mode.

Conclusion

A series of molecules having biguanide or dihydrotriazine pharmacophore were designed and synthesized as

potential inhibitors of DHFR. The synthesized molecules were tested as inhibitors of a number of pathogenic DHFRs such as *Pneumocystis carinii* (pc), *Toxoplasma gondii* (tg), and *Mycobacterium avium* (ma). Rat liver (rl) DHFR served as the mammalian standard to assess the selectivity. This series yielded two-digit nanomolar potency for seven compounds, against tgDHFR. One of the synthesized molecules, **B2-07**, showed similar potency to trimetrexate,

Table 2. Comparison of experimental binding energy with docking score.

Mol ID	tgDHFR activity, IC_{50} (μM)	ΔG_{expt}^a	XP			
			GScore ^a	Error ^a	Evdw ^a	Ecoul ^a
A1-01	40.265	-6.23	-7.49	-1.26	-46.30	-4.69
A1-02	135.465	-5.49	-7.49	-2.01	-45.47	-11.18
A1-03	145.281	-5.44	-8.52	-3.08	-47.53	-11.34
A2-01	0.424	-9.04	-5.24	3.80	-29.64	-7.69
A2-02	0.169	-9.61	-9.37	0.24	-30.30	-5.57
A2-03	0.079	-10.07	-11.46	-1.38	-45.17	-7.64
A2-04	0.523	-8.91	-11.95	-3.04	-42.65	-10.09
B1-01	131.649 (25)	>-5.50	-7.44	>1.93	-33.00	-7.22
B1-02	58.464	-6.00	-4.44	1.57	-40.30	-2.86
B1-03	9.948	-7.09	-7.39	-0.30	-34.24	-4.33
B1-04	111.146 (19)	>-5.61	-8.45	>2.84	-37.96	-8.41
B1-05	21.430	-6.62	-8.38	-1.76	-40.61	-6.49
B1-06	8.404	-7.20	-7.73	-0.53	-37.95	-5.85
B1-07	111.371	-5.61	-7.78	-2.17	-48.64	0.53
B2-01	0.032	-10.63	-9.01	1.62	-23.82	-5.52
B2-02	0.020	-10.92	-6.54	4.38	-28.92	-7.26
B2-03	0.040	-10.49	-9.19	1.31	-27.50	-3.95
B2-04	0.029	-10.69	-6.09	4.60	-30.10	-9.19
B2-05	0.033	-10.61	-10.73	-0.12	-38.50	-6.99
B2-06	0.019	-10.95	-10.02	0.93	-37.30	-5.87
B2-07	0.012	-11.23	-11.99	-0.75	-36.73	-5.83
Trimethoprim	2.800	-7.88	-10.08	-2.20	-32.29	-4.70
Piritrexim	0.0043	-11.87	-10.34	1.52	-35.69	-5.80
Trimetrexate	0.010	-11.35	-10.42	0.92	-36.08	-5.73

^aExperimental free energies from $\Delta G_{\text{expt}} = RT \ln IC_{50}$ in kcal/mol; XP Gscore, predicted binding energy using Glide in kcal/mol; Error (kcal/mol), difference between experimental and predicted binding energy from $\Delta G_{\text{expt}} - \text{XP GScore}$; Evdw and Ecoul, van der Waals and electrostatic interaction energies between ligand and receptor calculated using Glide.

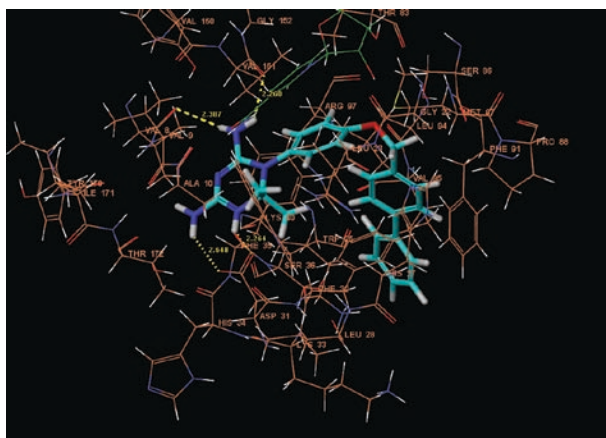


Figure 1. Binding mode of **B2-07** in the active site of developed tgDHFR homology model. Hydrogen bonding interactions are shown by yellow dotted lines, π - π stacking interaction with Phe91 is noticeable.

~233-fold improved potency compared with trimethoprim and ~7-fold increased selectivity as compared to trimetrexate against tgDHFR, indicating that this molecule could act as a good lead in the search for inhibitors with improved potency and better selectivity. This was further confirmed by molecular modeling studies. The results could be used for design and synthesis of analogs with improved potency and selectivity.

Declaration of interest: Seema Bag is thankful to University Grand Commission (UGC), India and Nilesh R. Tawari is thankful to Department of Biotechnology (DBT), India for financial support.

References

- Chan DCM, Anderson AC. Towards species-specific antifolates. *Curr Med Chem* 2006;13:377-98.
- Gangjee A, Kurup S, Namjoshi O. Dihydrofolate reductase as a target for chemotherapy in parasites. *Curr Pharm Design* 2007;13:609-39.
- Gangjee A, Yang J, Queener SF. Novel non-classical C9-methyl-5-substituted-2,4-diaminopyrrolo-[2,3-d]pyrimidines as potential inhibitors of dihydrofolate reductase and as anti-opportunistic agents. *Bioorg Med Chem* 2006;14:8341-51.
- Gangjee A, Adair OO, Pagley M, Queener SF. N9-substituted 2,4-diaminoquinazolines: synthesis and biological evaluation of lipophilic inhibitors of *Pneumocystis carinii* and *Toxoplasma gondii* dihydrofolate reductase. *J Med Chem* 2008;49:6195-200.
- Pelphrey PM, Popov VM, Joska TM, Beierlein JM, Bolstad ESD, Fillingham YA, et al. Highly efficient ligands for dihydrofolate reductase from *Cryptosporidium hominis* and *Toxoplasma gondii* inspired by structural analysis. *J Med Chem* 2007;50:940-50.
- Dasgupta T, Chitnumsub P, Kamchonwongpaisan S, Maneeruttanarungroj C, Nichols SE, Lyons TM, et al. Exploiting structural analysis, in silico screening, and serendipity to identify novel inhibitors of drug-resistant *falciparum* malaria. *ACS Chem Biol* 2009;4:29-40.
- Martucci WE, Udier-Blagovic M, Atreya C, Babatunde O, Vargo MA, Jorgensen WL, et al. Novel non-active site inhibitor of *Cryptosporidium hominis* TS-DHFR identified by a virtual screen. *Bioorg Med Chem Lett* 2009;19:418-23.
- Blaney JM, Hansch C, Silipo C, Vittoria A. Structure-activity relationships of dihydrofolate reductase inhibitors. *Chem Rev* 1984;84:333-407.
- Kidwai M, Mothra P, Mohan R, Biswas S. 1-Aryl-4,6-diamino-1,2-dihydrotriazine as antimalarial agent: a new synthetic route. *Bioorg Med Chem Lett* 2005;15:915-17.
- Baker BR, Janson EE. Irreversible enzyme inhibitors. CLV. Active-site-directed irreversible inhibitors of dihydrofolate reductase derived from 1-[4-omega-aminoalkoxy]-3-chlorophenyl]-4,6-diamino-1,2-dihydro-2,2-dimethyl-s-triazines bearing a terminal sulfonyl fluoride. *J Med Chem* 1969;12:672-6.
- Lee HK, Chui WK. Combinatorial mixture synthesis and biological evaluation of dihydrophenyl triazine antifolates. *Bioorg Med Chem* 1999;7:1255-62.
- Mayer S, Daigle DM, Brown ED, Khatri J, Organ MG. An expedient and facile one-step synthesis of a biguanide library by microwave irradiation coupled with simple product filtration. Inhibitors of dihydrofolate reductase. *J Comb Chem* 2004;6:776-82.
- Jensen NP, Ager AL, Bliss RA, Canfield CJ, Kotecka BM, Rieckmann KH, et al. Phenoxypyrimidopyrimidines, prodrugs of DHFR-inhibiting diaminotriazine antimalarials. *J Med Chem* 2001;44:3925-31 (and references therein).
- Broughton MC, Queener SF. *Pneumocystis carinii* dihydrofolate reductase used to screen potential antipneumocystis drugs. *Antimicrob Agents Chemother* 1991;35:1348-55.
- Chio LC, Queener SF. Identification of highly potent and selective inhibitors of *Toxoplasma gondii* dihydrofolate reductase. *Antimicrob Agents Chemother* 1993;37:1914-23.
- Kuyper L, Roth B, Baccanari D, Ferone R, Bedell CR, Campness JN, et al. Receptor-based design of dihydrofolate reductase inhibitors: comparison of crystallographically determined enzyme binding with enzyme affinity in a series of carboxy-substituted trimethoprim analogs. *J Med Chem* 1982;25:1120-3.
- Chan DCM, Fu H, Forsch RA, Queener SF, Rosowsky A. Design, synthesis, and antifolate activity of new analogues of piritrexim and other diaminopyrimidine dihydrofolate reductase inhibitors with omega-carboxyalkoxy or omega-carboxy-1-alkynyl substitution in the side chain. *J Med Chem* 2005;48:4420-31 (and references therein).
- Otzen T, Wempe EG, Kunz B, Bartels R, Lehwark-Yvetot G, Hänsel W, et al. Folate-synthesizing enzyme system as target for development of inhibitors and inhibitor combinations against *Candida albicans*—Synthesis and biological activity of new 2,4-diaminopyrimidines and 4'-substituted 4-aminodiphenyl sulfones. *J Med Chem* 2004;47:240-53.
- Bag S, Tawari NR, Degani MS. Insight into inhibitory activity of mycobacterial dihydrofolate reductase inhibitors by in-silico molecular modeling approaches. *QSAR Comb Sci* 2009;3:296-311.
- Allen CFH, Gates JW. *o-n*-Butoxynitrobenzene. *Organic Synth* 1945;25:9.
- Salzberg PL, Supniewski JV. beta-Bromoethylphthalimide. *Organic Synth* 1927;7:8.
- Baker BR, Ho B-T. Analogs of tetrahydrofolic acid. xxix. Hydrophobic bonding to dihydrofolate reductase. ii. On the mode of phenyl binding of 1-aryl-4,6-diamino-1,2-dihydro-2,2-dimethyl-s-triazines. *J Heterocycl Chem* 1965;2:335-9.
- Modest EJ. Chemical, and biological studies on 1,2-dihydro-s-triazines., II. Three-component synthesis. *J Org Chem* 1956;21:1-13.
- Glide, version 5.0. New York: Schrödinger, LLC, 2008.
- LigPrep, version 3.0. New York: Schrödinger, LLC, 2008..